

# CrystEngComm

Accepted Manuscript



This is an *Accepted Manuscript*, which has been through the Royal Society of Chemistry peer review process and has been accepted for publication.

*Accepted Manuscripts* are published online shortly after acceptance, before technical editing, formatting and proof reading. Using this free service, authors can make their results available to the community, in citable form, before we publish the edited article. We will replace this *Accepted Manuscript* with the edited and formatted *Advance Article* as soon as it is available.

You can find more information about *Accepted Manuscripts* in the [Information for Authors](#).

Please note that technical editing may introduce minor changes to the text and/or graphics, which may alter content. The journal's standard [Terms & Conditions](#) and the [Ethical guidelines](#) still apply. In no event shall the Royal Society of Chemistry be held responsible for any errors or omissions in this *Accepted Manuscript* or any consequences arising from the use of any information it contains.

**Exploring supramolecular assembly and luminescent behavior in a series of RE-*p*-chlorobenzoic acid-1,10-phenanthroline complexes**Korey P. Carter<sup>§</sup>, Cecilia H. F. Zulato<sup>§,†</sup> and Christopher L. Cahill\*<sup>§</sup><sup>§</sup> Department of Chemistry, The George Washington University, 725 21<sup>st</sup> Street, NW, Washington, D.C. 20052, United States<sup>†</sup> Laboratory of Functional Materials, Institute of Chemistry, University of Campinas, UNICAMP, P. O. Box 6154, Campinas, Sao Paulo, Brazil, 13083-970**Abstract**

Eleven new rare earth (RE) *p*-chlorobenzoic acid-1,10-phenanthroline complexes have been hydrothermally synthesized and structurally characterized via single-crystal and powder X-ray diffraction. This series builds on four previous single complex studies to analyze the structural, supramolecular and luminescent properties of the set of binuclear molecular complexes that are formed with all members of the lanthanide series and yttrium (La-Y). All complexes discussed herein feature a bidentate phenanthroline ligand, *p*-chlorobenzoic acid ligands exhibiting multiple bind modes, chelating-bridging bidentate, bridging bidentate, bidentate and monodentate, and for the larger Ln<sup>3+</sup> ions (La-Nd) a bound water molecule. Supramolecular assembly yields 2D sheets for all the binuclear species with Cl- $\pi$ ,  $\pi$ - $\pi$  and hydrogen bonding interactions simultaneously present in structure type I,  $\pi$ - $\pi$  and hydrogen bonding assembling the binuclear tectons in structure type II and a combination of Cl- $\pi$  and  $\pi$ - $\pi$  interactions stitching together the dimer units of structure type III. Visible luminescence experiments were performed on the Pr, Sm, Dy and Tm materials and the results ranged from complete sensitization for Sm and Dy to incomplete energy transfer in the Tm complex, and a complete absence of luminescence in the Pr material.

## Introduction

The study of rare-earth materials incorporating conjugated carboxylic acids is a diverse area of structural chemistry and compounds displaying a rich array of coordination types have been recognized.<sup>1-5</sup> Rare earth-carboxylate hybrid materials (coordination polymers, MOFs) have garnered much of the attention thus far as the covalent coordination of multifunctional carboxylic acid ligands has generated many extended topologies<sup>6-9</sup> with a range of potential applications including gas storage<sup>10, 11</sup> sensing<sup>12</sup> and separations.<sup>13</sup> On the other hand, *molecular* lanthanide complexes containing aromatic carboxylic acids remain a topic of fundamental interest as these materials have been utilized in a wide variety of applications including electroluminescent materials,<sup>14, 15</sup> luminescent bioprobes<sup>16</sup> and non-linear optics.<sup>17, 18</sup> Recent studies have also shown that Ln(III) molecular complexes exhibit particular promise in the development of materials that display single-ion and single molecule magnetic properties.<sup>19-21</sup>

Lanthanide luminescence is indeed a topic of great interest due to the unique nature of Ln(III) emission, originating from the core-like 4f orbitals of the Ln<sup>3+</sup> metal ions.<sup>22</sup> Direct excitation of lanthanide metal centers is hindered by small absorption cross-sections, low molar absorption coefficients and the nature of f-f electronic transitions, which are formally Laporte forbidden.<sup>23</sup> A popular alternative to direct excitation of Ln(III) metal centers is the well-known antenna effect, which involves the efficient absorption of incident light via an organic chromophore and the corresponding sensitization of the Ln(III) metal ion via ligand to metal energy transfer.<sup>24, 25</sup> Efficient utilization of the antenna effect requires the selection of organic chromophores with

triplet states energies in the appropriate range for sensitization of the corresponding lanthanide ions, and with this key criterion in mind we selected the ligands used herein for the assembly of a series of luminescent lanthanide molecular complexes.

The bidentate N-donor 1,10-phenanthroline (“phen”) is a versatile starting material for inorganic and supramolecular synthesis. Phen is a rigid, planar, electron-poor heteroaromatic system with nitrogen atoms ideally placed for cation binding.<sup>26</sup> In aqueous solution, phen behaves as a weak base, yet despite its protonation constant (basicity) being only 4.95 log units,<sup>27</sup> phen shows a moderate affinity for binding Ln(III) ions due to its preorganization.<sup>28</sup> A search of the Cambridge Structural Database (CSD, V. 5.35, Nov. 2013)<sup>29</sup> reveals 1156 compounds that feature both a lanthanide metal ion and phen. Narrowing this search to include an aromatic carboxylate drops the number of complexes to 352, illustrating that the use of phen as a co-ligand in molecular lanthanide complexes with aromatic carboxylic acids is well established.<sup>30</sup> A more detailed look at these 352 complexes reveals that the use of phen as a co-ligand with the intent of ‘capping’ one side of the coordination sphere was first reported in the pioneering works of White *et. al.*<sup>31</sup> and a significant amount of exploration has followed including four structures where phen and *p*-chlorobenzoic acid were used together.<sup>21, 32-35</sup>

Whereas the use of bidentate capping ligands (i.e. phen) is indeed mature and well explored from a coordination chemistry perspective, our own efforts in hydro(solvo)thermal formation of hybrid materials have a bit more of a targeted, crystal engineering approach. For instance, hydrothermal synthesis of Ln(III) bearing MOF and coordination polymer structures often contain polynuclear secondary building units (SBU) or clusters resulting from lanthanide ion hydrolysis.<sup>36, 37</sup> Subsequently, minimal

control is afforded over speciation and ultimately, extended solid-state structures. Work has been done in our group recently where 2,2':6',2''-terpyridine (“terpy”) was used as a capping ligand with the *direct goal* of controlling oligomerization and a series of molecular materials with *p*-chlorobenzoic acid was synthesized, and various means of supramolecular assembly were explored.<sup>38</sup> The work outlined herein acts as a follow up investigation and like our work with terpy, is a systematic study across the complete Ln<sup>3+</sup> series. Despite numbers suggesting that the use of phen in lanthanide materials with aromatic carboxylates is well explored, out of the 352 CSD entries mentioned above, one finds only two systematic single crystal XRD studies (works including at least six of the fourteen lanthanide metals).<sup>39, 40</sup> Moreover, the selection of a chelating ligand, such as phen, with the direct goal of thwarting Ln(III) hydrolysis and acting as structure directing tool for crystal engineering was introduced in our previous work,<sup>38</sup> but is not a concept that has been explored explicitly within the lanthanide series in any sort of systematic fashion. As such, the approach adopted herein is to generate a molecular Ln(III) complex (or ‘tecton’) which will then be assembled through supramolecular interactions (‘synthons’) made possible by the various functional groups at the complex’s periphery.

The construction of extended solid-state structures via supramolecular assembly utilizes the diverse array of synthons that have been discovered,<sup>41, 42</sup> and the use of these supramolecular building blocks as a means of assembling molecular units into extended structures has been well studied in the d-metal-organic systems,<sup>43-45</sup> and in our group with the uranyl cation.<sup>46-48</sup> Supramolecular synthons involving the halogens are of particular interest to our group due to their ability to participate in interactions with other halogens, cations and anions and herein we will highlight a lesser-developed area of assembly

utilizing halogen- $\pi$  interactions. Up to this point, most examples of assembly via halogen- $\pi$  synthons have taken place in strictly organic systems,<sup>49-51</sup> although recent works have started to look at these synthons in metal-organic systems.<sup>38, 52, 53</sup> The significance of supramolecular interactions in lanthanide molecular systems has been discussed for systems utilizing hydrogen bonding and  $\pi$ - $\pi$  stacking,<sup>54-57</sup> and in a recent example of assembly via anion- $\pi$  interactions,<sup>58</sup> yet lanthanide supramolecular assembly remains an area that warrants further investigation as the mechanisms for the promotion of extended structures with desired geometries remains elusive.

Herein we report the synthesis, crystal structures, supramolecular interactions and luminescent properties (where they have not been covered previously) of a family of eleven homodinuclear rare earth molecular materials containing the organic ligands *p*-chlorobenzoic acid and 1,10-phenanthroline. One of these complexes is a new structure (complex **1** with La), whereas the other ten are new isomorphs of two previously characterized compounds  $([\text{Pr}(\text{C}_{12}\text{H}_8\text{N}_2)(\text{C}_7\text{H}_4\text{ClO}_2)_3(\text{H}_2\text{O})]_2, [\text{Ln}(\text{C}_{12}\text{H}_8\text{N}_2)(\text{C}_7\text{H}_4\text{ClO}_2)_3]_2$ -(where Ln=Eu, Tb, Dy)).<sup>34, 35</sup> Each complex features a fixed local geometry where supramolecular interactions ( $\pi$ - $\pi$ , hydrogen bonding or halogen- $\pi$ ) outside the immediate  $\text{RE}^{3+}$  coordination sphere are used to stitch together the molecular tectons into extended solid-state structures of varying dimensionality. Moreover, this systematic study of molecular lanthanide materials that incorporate both *p*-chlorobenzoic acid and phen highlights the effects of the lanthanide contraction on local and global structure across the entirety of the RE(III) series from La-Y, with the exception of Pm. In particular, we note an evolution in modes of supramolecular assembly that results directly

from the nature of local geometry of the first coordination sphere of the RE<sup>3+</sup> metal center.

## Experimental Section

### Materials and Methods

La(NO<sub>3</sub>)<sub>3</sub>•6H<sub>2</sub>O (Strem Chemicals, 99.9%), Ce(NO<sub>3</sub>)<sub>3</sub>•6H<sub>2</sub>O (Sigma Aldrich, 99%), Pr(NO<sub>3</sub>)<sub>3</sub>•6H<sub>2</sub>O (Strem Chemicals, 99.9%) Nd(NO<sub>3</sub>)<sub>3</sub>•6H<sub>2</sub>O (Sigma Aldrich, 99.9%), Sm(NO<sub>3</sub>)<sub>3</sub>•6H<sub>2</sub>O (Alfa Aesar, 99.9%), Ln(NO<sub>3</sub>)<sub>3</sub>•xH<sub>2</sub>O (where Ln=Eu, Gd, Tb, Dy, Ho, Er, Yb and Y, x=1,5 or 6, Strem Chemicals, 99.9%), Ln(NO<sub>3</sub>)<sub>3</sub>•xH<sub>2</sub>O (where Ln=Tm, Lu, x=1 or 5, Sigma Aldrich, 99.9%), *p*-chlorobenzoic acid (Sigma Aldrich, 99%), and 1,10-phenanthroline (Alfa Aesar, Fischer, 98%) were used for syntheses as received.

### Synthesis

Complexes **1-11** discussed herein were all synthesized via hydrothermal methods in a 23 mL Teflon-lined autoclave at an oven temperature of 120 °C.

A mixture of Ln<sup>3+</sup> nitrate hydrate (Ln(NO<sub>3</sub>)<sub>3</sub>•xH<sub>2</sub>O, Ln=La-Y, x=1, 5 or 6), *p*-chlorobenzoic acid (C<sub>7</sub>H<sub>4</sub>ClO<sub>2</sub>), 1, 10-phenanthroline (C<sub>12</sub>H<sub>8</sub>N<sub>2</sub>) and distilled water (molar ratio 1:2:2:826) was heated for 48 hours under autogenous pressure. Upon removal from the oven, the samples were allowed to cool to ambient temperature over four hours and then opened after approximately twelve hours. Colorless or pink, in the case of Ho and Er, plate-like crystals were obtained from the bulk product after decanting the supernatant liquor, washing twice with distilled water and ethanol, and air-drying at room temperature.

Whereas the Pr, Eu, Tb and Dy members of this series have been made previously via solvothermal methods,<sup>21, 32-35</sup> they were re-synthesized in this study using the above method to allow for further characterization of these materials.

## Characterization

### X-Ray Structure Determination

Single crystals from each bulk sample were isolated and mounted on MiTeGen micromounts. Structure determination for each of the single crystals was achieved by collecting reflections using  $0.5^\circ \omega$  scans on a Bruker SMART diffractometer furnished with an APEX II CCD detector using  $\text{MoK}\alpha$  ( $\lambda=0.71073 \text{ \AA}$ ) radiation at room temperature (293 K). Integration was done using the *SAINTE* software package<sup>59</sup> that is a part of the APEX II software suite<sup>60</sup> and absorption corrections were conducted using *SADABS*.<sup>61</sup> Complexes **1**, **2**, **4**, **5**, **7**, **8**, **9**, **10** and **11** were solved via direct methods using *SIR 92*<sup>62</sup> and complexes **3** and **6** were solved via the Patterson Method (*SHELXS-2013*).<sup>63</sup> All eleven complexes were refined using *SHELXL-2013*<sup>63</sup> in the *WinGX*<sup>64</sup> software suite. In each structure, all non-hydrogen atoms were located via difference Fourier maps and refined anisotropically. Aromatic hydrogen atom positions were placed at their idealized positions by employing the HFIX43 instruction in *SHELXL-2013* and allowed to ride on the coordinates of the parent atom with isotropic thermal parameters ( $U_{iso}$ ) fixed at  $1.2U_{eq}$  of the carbon atom to which they are attached. In structures **1-3**, the hydrogen atoms (HW1 and HW2) on the  $\text{Ln}^{3+}$  bound water molecule were located via difference Fourier map and modeled with DFIX restraints which placed the H atoms at calculated distances. Structures were checked for additional symmetry using *PLATON*.<sup>65</sup> All figures were

prepared with CrystalMaker.<sup>66</sup> Data collection and refinement details for complexes **1-11** are included in Table 1.

### **Powder X-ray Diffraction**

Powder X-ray diffraction (PXRD) data on the bulk reaction product of complexes **1-11** (Figures S1-S11, Supporting Information) were used to examine the bulk purity of each sample. For the previously reported Pr, Eu, Tb and Dy materials that were re-made as a part of this study, PXRD data was used to confirm that the materials had been successfully reproduced (Figures S12-S15, Supporting Information). All data were collected on a Rigaku Miniflex (Cu K $\alpha$ , 2 $\theta$ =3-60°) and were analyzed using the JADE software program.<sup>67</sup> The bulk products of **2**, **3** and **6** contain minor impurities that could not be identified.

### **Luminescence Measurements**

Room temperature solid-state luminescence measurements were obtained for the Pr, Sm, Dy and Tm complexes on a Horiba JobinYvon Fluorlog-3 spectrophotometer. All data were manipulated using the FluoroEssence software package and final plots of the solid-state spectra were made in Microsoft Excel. For each sample, approximately ten milligrams of material was gently ground into a fine powder with a mortar and pestle. Eight drops of cyclohexane were added and the resulting slurry which was then added dropwise to a microscope slide. Drops were focused on a targeted area in the center of the microscope slide with the goal of concentrating the sample in order to optimize the luminescent spectra. After all solid material had been carefully added to the microscope slide, the samples were allowed to air dry for approximately ten minutes at which point a cover slide was placed on top of the sample and secured with adhesive tape.

**Table 1:** Crystallographic Data for Compound **1-11**

	<b>1 (I)</b>	<b>2 (II)</b>	<b>3 (II)</b>	<b>4 (III)</b>
chem formula	C <sub>66</sub> H <sub>44</sub> Cl <sub>6</sub> N <sub>4</sub> O <sub>14</sub> La <sub>2</sub>	C <sub>66</sub> H <sub>44</sub> Cl <sub>6</sub> N <sub>4</sub> O <sub>14</sub> Ce <sub>2</sub>	C <sub>66</sub> H <sub>44</sub> Cl <sub>6</sub> N <sub>4</sub> O <sub>14</sub> Nd <sub>2</sub>	C <sub>66</sub> H <sub>40</sub> Cl <sub>6</sub> N <sub>4</sub> O <sub>12</sub> Sm <sub>2</sub>
formula weight	1607.57	1609.99	1618.23	1594.42
cryst system	triclinic	triclinic	triclinic	triclinic
space group	P-1	P-1	P-1	P-1
<i>a</i> (Å)	10.0914(5)	8.4595(5)	8.4411(3)	10.0492(4)
<i>b</i> (Å)	12.6143(6)	12.9231(8)	12.9074(4)	11.9135(5)
<i>c</i> (Å)	13.2987(6)	15.4404(9)	15.4508(5)	14.3855(6)
$\alpha$ (deg)	99.312(3)	98.995(6)	98.976(1)	110.397(2)
$\beta$ (deg)	100.740(4)	100.654(7)	100.829(1)	96.364(3)
$\gamma$ (deg)	96.354(4)	100.680(6)	100.727(2)	102.190(2)
<i>V</i> (Å <sup>3</sup> )	1623.89(14)	1598.09(17)	1592.40(9)	1545.56(11)
<i>Z</i>	1	1	1	1
<i>T</i> (K)	293	293	293	293
$\lambda$ (Mo K $\alpha$ )	0.71073	0.71073	0.71073	0.71073
<i>D</i> <sub>calc</sub> (g cm <sup>-3</sup> )	1.644	1.673	1.687	1.713
$\mu$ (mm <sup>-1</sup> )	1.613	1.726	1.933	2.208
<i>R</i> <sub>int</sub>	0.0451	0.0530	0.0443	0.0248
<i>R</i> <sub>1</sub> [ <i>I</i> > 2 $\sigma$ ( <i>I</i> )]	0.0347	0.0384	0.0370	0.0213
w <i>R</i> <sub>2</sub> [ <i>I</i> > 2 $\sigma$ ( <i>I</i> )]	0.0659	0.0755	0.0716	0.0523
	<b>5 (III)</b>	<b>6 (III)</b>	<b>7 (III)</b>	<b>8 (III)</b>
chem formula	C <sub>66</sub> H <sub>40</sub> Cl <sub>6</sub> N <sub>4</sub> O <sub>12</sub> Gd <sub>2</sub>	C <sub>66</sub> H <sub>40</sub> Cl <sub>6</sub> N <sub>4</sub> O <sub>12</sub> Ho <sub>2</sub>	C <sub>66</sub> H <sub>40</sub> Cl <sub>6</sub> N <sub>4</sub> O <sub>12</sub> Er <sub>2</sub>	C <sub>66</sub> H <sub>40</sub> Cl <sub>6</sub> N <sub>4</sub> O <sub>12</sub> Tm <sub>2</sub>
formula weight	1608.22	1623.58	1628.24	1631.58
cryst system	triclinic	triclinic	triclinic	triclinic
space group	P-1	P-1	P-1	P-1
<i>a</i> (Å)	10.0755(3)	10.0939(3)	10.0959(3)	10.1079(3)
<i>b</i> (Å)	11.8866(3)	11.8412(4)	11.8279(3)	11.8190(3)
<i>c</i> (Å)	14.3488(4)	14.2899(5)	14.2740(4)	14.2667(4)
$\alpha$ (deg)	110.75(3)	111.041(2)	111.186(9)	111.320(2)
$\beta$ (deg)	96.41(3)	96.482(1)	96.461(9)	96.529(3)

$\gamma$ (deg)	101.87(2)	101.468(1)	101.386(11)	101.207(2)
$V$ ( $\text{\AA}^3$ )	1540.3(4)	1530.24(9)	1526.17(7)	1525.43(8)
$Z$	1	1	1	1
$T$ (K)	293	293	293	293
$\lambda$ (Mo K $\alpha$ )	0.71073	0.71073	0.71073	0.71073
$D_{\text{calc}}$ (g $\text{cm}^{-3}$ )	1.734	1.762	1.772	1.776
$\mu$ ( $\text{mm}^{-1}$ )	2.462	2.896	3.061	3.220
$R_{\text{int}}$	0.0270	0.0286	0.0271	0.0300
R1 [ $I > 2\sigma(I)$ ]	0.0249	0.0258	0.0236	0.0267
wR2 [ $I > 2\sigma(I)$ ]	0.0539	0.0541	0.0515	0.0586
	<b>9 (III)</b>	<b>10 (III)</b>	<b>11 (III)</b>	
chem formula	$\text{C}_{66}\text{H}_{40}\text{Cl}_6\text{N}_4\text{O}_{12}\text{Yb}_2$	$\text{C}_{66}\text{H}_{40}\text{Cl}_6\text{N}_4\text{O}_{12}\text{Lu}_2$	$\text{C}_{66}\text{H}_{40}\text{Cl}_6\text{N}_4\text{O}_{12}\text{Y}_2$	
formula weight	1639.80	1643.66	1471.54	
cryst system	triclinic	triclinic	triclinic	
space group	P-1	P-1	P-1	
$a$ ( $\text{\AA}$ )	10.0937(8)	10.1082(5)	10.0929(8)	
$b$ ( $\text{\AA}$ )	11.8057(9)	11.7926(5)	11.8472(9)	
$c$ ( $\text{\AA}$ )	14.2502(11)	14.2440(7)	14.2880(11)	
$\alpha$ (deg)	111.386(5)	111.419(3)	111.160(3)	
$\beta$ (deg)	96.465(4)	96.559(3)	96.429(4)	
$\gamma$ (deg)	101.209(5)	101.088(2)	101.497(4)	
$V$ ( $\text{\AA}^3$ )	1519.4(2)	1519.19(13)	1529.3(2)	
$Z$	1	1	1	
$T$ (K)	293	293	293	
$\lambda$ (Mo K $\alpha$ )	0.71073	0.71073	0.71073	
$D_{\text{calc}}$ (g $\text{cm}^{-3}$ )	1.792	1.797	1.598	
$\mu$ ( $\text{mm}^{-1}$ )	3.391	3.562	2.218	
$R_{\text{int}}$	0.0371	0.0653	0.0534	
R1 [ $I > 2\sigma(I)$ ]	0.0284	0.0407	0.0422	
wR2 [ $I > 2\sigma(I)$ ]	0.0586	0.0661	0.0830	

## Results

### Description of Structures

Single crystal X-ray crystallography analyses yielded three unique structure types in this series of molecular complexes. Each structure type can be described as binuclear species and a representative structural example (**1**, **3** and **9**) will be presented in detail.

#### [La(C<sub>12</sub>H<sub>8</sub>N<sub>2</sub>)(C<sub>7</sub>H<sub>4</sub>ClO<sub>2</sub>)<sub>3</sub>(H<sub>2</sub>O)]<sub>2</sub>-(**1**)-Structure Type I

Complex **1** is a new structure and crystallizes in the triclinic space group P-1 and has an asymmetric unit containing a single unique La<sup>3+</sup> ion bound by a bidentate phen, a bound water molecule and three *p*-chlorobenzoic acid ligands adopting three different coordination modes: chelating-bridging bidentate, bridging bidentate and monodentate (Figure 1). The La<sup>3+</sup> metal center has a coordination number of nine and adopts a distorted monocapped square antiprismatic molecular geometry. La1-O bond distances for the chelating-bridging bidentate *p*-chlorobenzoic acid (O1 and O2) are 2.542(2) Å and 2.517(2) Å, respectively. The bridging interaction from O2 to the La<sup>3+</sup> symmetry equivalent (La1'), this is the bridging component of the chelating-bridging behavior, is at a distance of 2.818(2) Å. The lanthanum metal center (La1) and its symmetry equivalent are further connected via a bridging bidentate *p*-chlorobenzoic acid (O3 and O4) to form a binuclear molecular tecton with La<sup>3+</sup>-oxygen distances of 2.517(2) Å to O3 and 2.437(2) Å to O4. A third *p*-chlorobenzoic acid ligand adopts the monodentate-binding mode via O5 and the La1-O5 distance is 2.466(2) Å. The bound water, OW1, is at a bond distance of 2.5551(2) Å from the La<sup>3+</sup> metal center and facilitates intermolecular hydrogen bonding interactions, which will be discussed in detail below. A chelating bidentate phen molecule (N1 and N2) completes the coordination sphere of the nine-

coordinate  $\text{La}^{3+}$  metal center with La-N distances of 2.758(2) Å to N1 and 2.743(2) Å to N2.

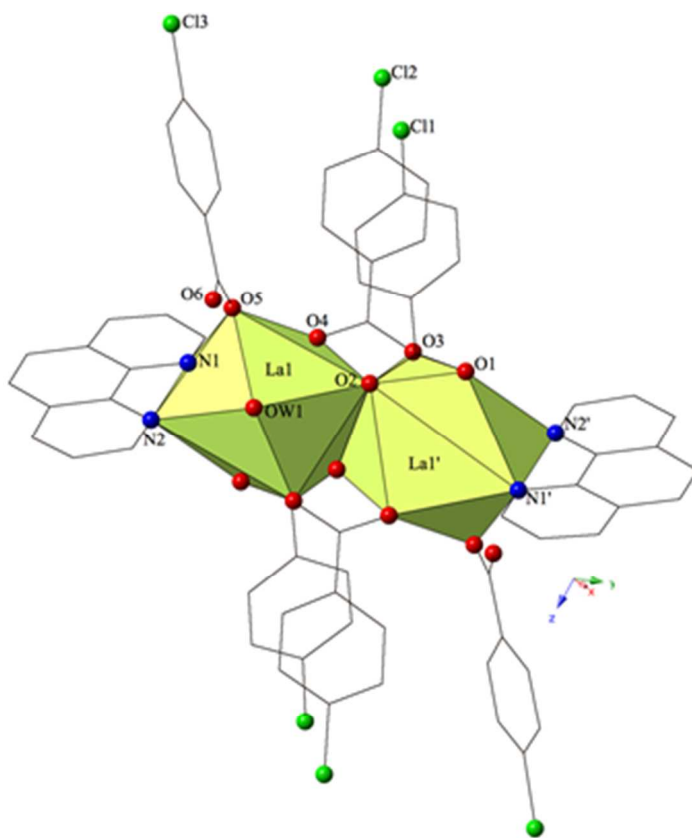


**Figure 1** Polyhedral representation of structure type I. Yellow polyhedra are  $\text{La}^{3+}$  metal centers, whereas spheres represent chlorine (green), nitrogen (blue) and oxygen (red). All H atoms have been omitted for clarity.

The binuclear molecular tectons of complex **1** are stitched together to form a supramolecular 1D chain along approximately the [001] direction via two independent and moderately strong<sup>68</sup> localized Cl- $\pi$  (Cl2-C10) and (Cl3-C2) interactions<sup>69</sup> between two *p*-chlorobenzoic acid ligands on the same lanthanum binuclear unit with phenanthroline ligands on two neighboring units (Figure 2a). Halogen- $\pi$  interactions are defined as moderate to strong lone pair- $\pi$  interactions by Reedijk *et. al.*<sup>68</sup> based on whether they are less than or equal to the corresponding sum of the van der Waals radii

(3.450 Å for chlorine and carbon). There are interactions between the chlorine (Cl2) of one *p*-chlorobenzoic acid with the edge of a phenanthroline unit (C10) on a neighboring unit at a distance of 3.407(4) Å, and then a second interaction from the chlorine (Cl3) of another *p*-chlorobenzoic ligand to the edge of a different neighboring phenanthroline unit (C2) at a distance of 3.423(4) Å. Both of these interactions are well within the sum of the corresponding vdW radii of chlorine and carbon which suggests that vdW overlap of the chlorine atoms and the aromatic rings in structure **I** are significant.

The binuclear molecular tectons of complex **1** are further assembled to form a 2D sheet in the (011) plane via slightly offset  $\pi$ - $\pi$  stacking interactions<sup>70</sup> between phenanthroline ligands on neighboring units (Figure 2b). These non-covalent interactions are between the centroid of the phen moiety on one unit with the edge of the phen ring on the neighboring unit. The relevant distances and angles for these interactions are: Cg...Cg...3.667(2) Å; Cg $\perp$ ...Cg $\perp$ ...3.3947(14) Å;  $\beta$ =22.23°.

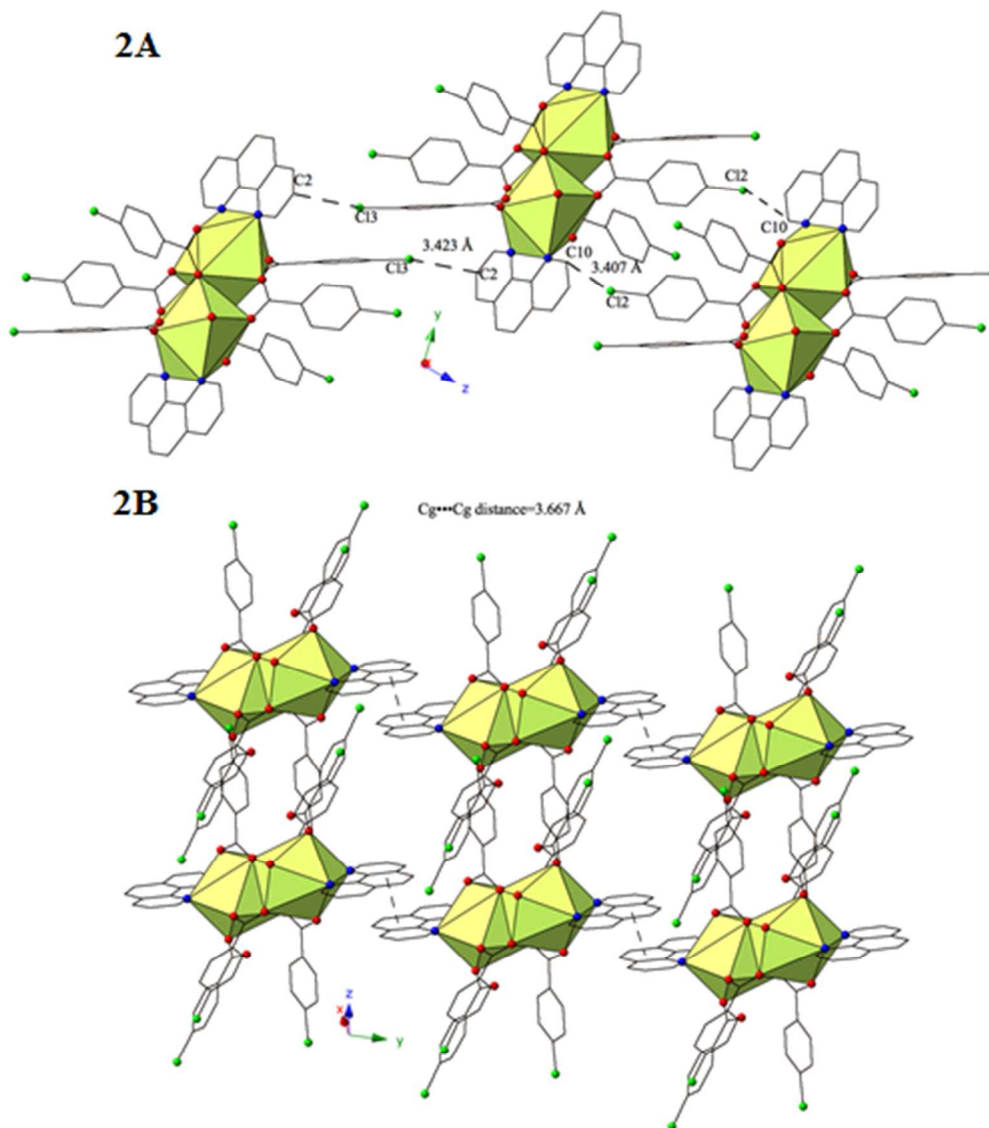


**Figure 2** a) Polyhedral representation of structure type I viewed down the [001] direction. Cl- $\pi$  interactions that link together binuclear units to form 1D chain are shown. b)  $\pi$ - $\pi$  interactions that assemble tectons into 2D sheets in the (011) plane.

### $[\text{Ln}(\text{C}_{12}\text{H}_8\text{N}_2)(\text{C}_7\text{H}_4\text{ClO}_2)_3(\text{H}_2\text{O})]_2$ -(where Ln=Ce, Nd) (2 and 3)-Structure Type II

The local structure of structure type II has briefly been described previously<sup>34</sup> and is included here in more detail. Single crystal X-ray diffraction analysis reveals that complexes **2** and **3** are isomorphous and crystallize in the triclinic space group P-1. As such, only the Nd complex (**3**) will be described here in detail. The asymmetric unit of

complex **3** contains a single crystallographically unique Nd<sup>3+</sup> ion coordinated by a bidentate phen, a bound water molecule and three *p*-chlorobenzoic acid ligands adopting either a bridging bidentate or monodentate coordination mode (Figure 3). The eight-coordinate Nd<sup>3+</sup> metal center also adopts a distorted square antiprismatic molecular geometry. Nd1-O bond distances for the bridging bidentate *p*-chlorobenzoic acid groups (O1, O2, O3 and O4) are 2.419(2) Å, 2.4394(19) Å, 2.456(2) Å and 2.3995(19) Å respectively. These two bridging carboxylate groups connect the Nd<sup>3+</sup> metal center and its symmetry equivalent to form a binuclear molecular dimer. A monodentate *p*-chlorobenzoic acid (O5) is also coordinated to the neodymium metal center and the Nd1-O5 bond distance is 2.408(2) Å, whereas the coordinated water molecule, OW1, has a Nd1-OW1 bond distance of 2.488(2) Å. This water molecule facilitates further intermolecular interactions via hydrogen bonding, which will be discussed in the following paragraph. Completing the coordination sphere of the neodymium is a bidentate phen molecule, which is bound through its two nitrogen atoms (N1 and N2) and the Nd1-N distances are 2.678(2) Å to N1 and 2.650(3) Å to N2, respectively.

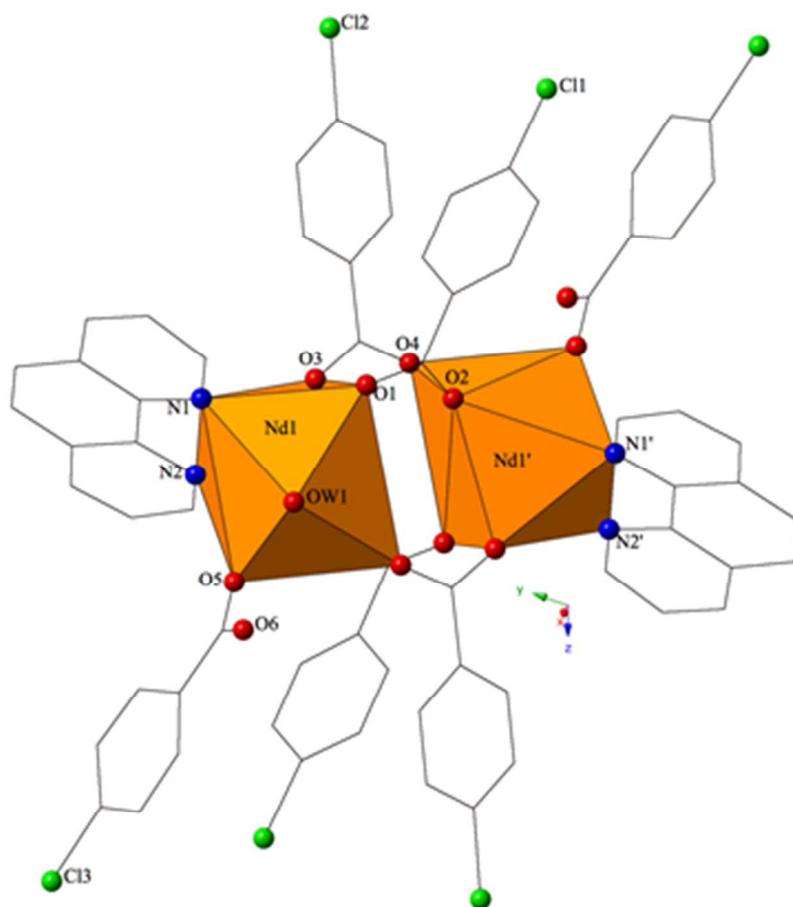


**Figure 3** Polyhedral representation of structure type II. Orange polyhedra are  $\text{Nd}^{3+}$  metal centers. All H atoms have been omitted for clarity.

A bifurcated hydrogen bonding interaction tethers the Nd binuclear units along the [100] direction resulting in a supramolecular 1D chain. (Figure 4a) These H-bonding interactions originate from the bound water, OW1, which links with the free carboxylate oxygen, O6, on the same  $\text{Nd}^{3+}$  metal at a distance of 2.616(3) Å and to the bridging bidentate bound carboxylate oxygen, O2, on the symmetry equivalent of the  $\text{Nd}^{3+}$  metal center at a slightly longer distance of 2.838(3) Å.

The binuclear molecular tectons of complex **3** are further assembled to form a 2D sheet in the (011) plane via slightly offset  $\pi$ - $\pi$  stacking interactions between phenanthroline ligands on neighboring units (Figure 4b). These non-covalent interactions

are between the centroid of the phen moiety on one unit with the edge of the phen ring on the neighboring unit. The relevant distances and angles for these interactions are:  $Cg \cdots Cg \cdots 3.739(2) \text{ \AA}$ ;  $Cg \perp \cdots Cg \perp \cdots 3.3722(15) \text{ \AA}$ ;  $\beta = 23.41^\circ$ .

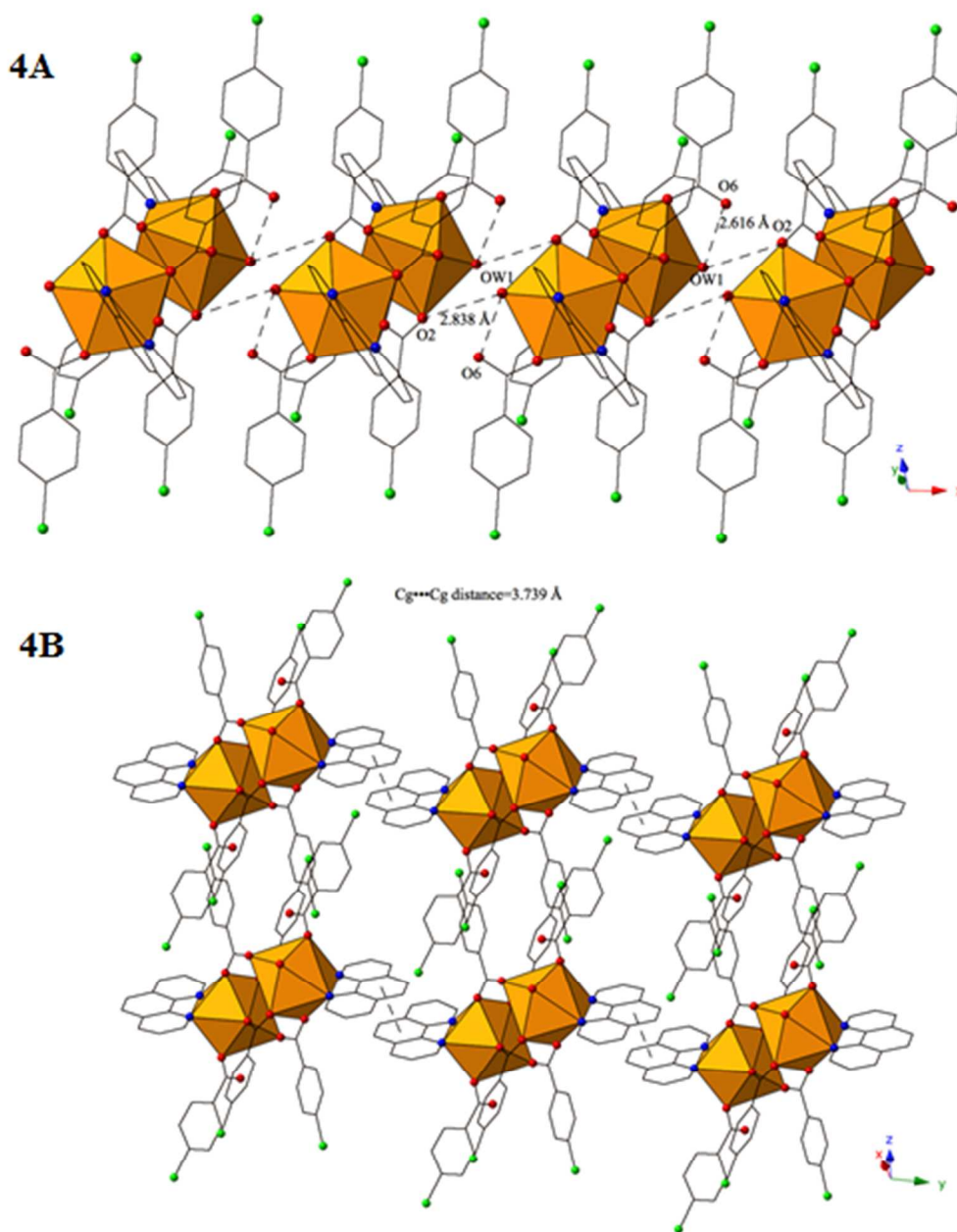


**Figure 4a)** Polyhedral representation of structure type II highlighting chains that propagate along the [100] direction. Bifurcated hydrogen bonding interactions that stitch together binuclear units to form 1D chain are shown. **b)**  $\pi$ - $\pi$  interactions that assemble tectons into 2D sheets in the (011) plane.

**[Ln(C<sub>12</sub>H<sub>8</sub>N<sub>2</sub>)(C<sub>7</sub>H<sub>4</sub>ClO<sub>2</sub>)<sub>3</sub>]<sub>2</sub>-(where Ln=Sm, Gd, Ho-Y) (4-11)-Structure Type III**

The structural details of structure type III have been described previously for the Eu, Tb and Dy isomorphs<sup>21, 32, 33, 35</sup> of complexes **4-11**. Each of eight new isomorphs presented herein crystallize in the triclinic space group P-1 and for completeness, the Yb complex (**9**) will be used as representative example and will be described here in detail. The asymmetric unit of complex **9** contains a Yb<sup>3+</sup> metal center that is coordinated to three *p*-chlorobenzoic acid ligands in either a bridging bidentate or bidentate configuration and a bidentate phen. The Yb<sup>3+</sup> metal center is eight-coordinate and adopts a distorted square antiprismatic molecular geometry (Figure 5). The average ytterbium-oxygen bond distance for the bridging bidentate *p*-chlorobenzoic acid ligands (O3, O4, O5, and O6) is 2.270 Å. For the bidentate *p*-chlorobenzoic acid, the Yb1-O distance is 2.314(2) Å to O1 and 2.453(2) Å to O2. These values are slightly shorter than those reported for the similar binuclear species discussed previously (Structure Type II) but these differences are likely the result of smaller ionic radius of Yb<sup>3+</sup> (compared to Nd<sup>3+</sup>). Yb<sup>3+</sup>-N bond distances (N1 and N2) for the phen molecule are 2.581(2) Å to N1 and 2.509(2) to N2 respectively.

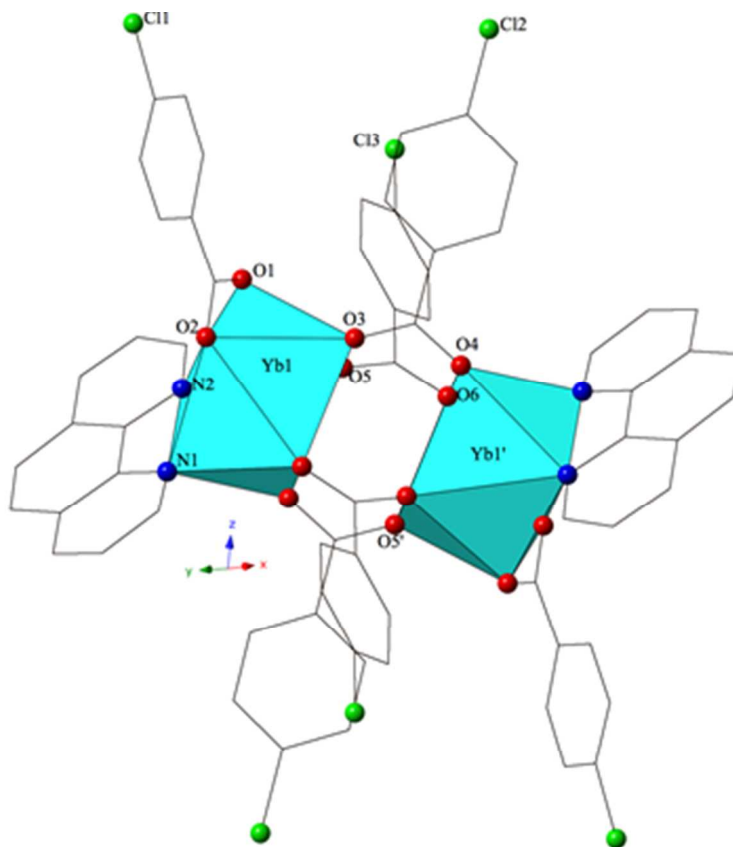


**Figure 5** Polyhedral representation of structure type III. Turquoise polyhedra are  $\text{Yb}^{3+}$  metal centers. All H atoms have been omitted for clarity.

The binuclear molecular tectons of complex **9** are linked to form a supramolecular 1D chain propagating in the  $[010]$  direction via strong<sup>68</sup> localized Cl- $\pi$  (C11-C25) interactions between *p*-chlorobenzoic acid ligands on neighboring units (Figure 6a). The interactions between the chlorine (C11) of one *p*-chlorobenzoic acid with the periphery of the benzene ring of a *p*-chlorobenzoic acid ligand (C25) on the neighboring unit are at a distance of 3.268(5) Å, which is well within the sum of the corresponding vdW.

The binuclear units of complex **9** are assembled into supramolecular 2D sheets in the (011) plane by slightly offset  $\pi$ - $\pi$  stacking interactions between phen moieties that act in concert with the Cl- $\pi$  interactions discussed above. (Figure 6b) The center of the

aromatic ring of one phen unit overlaps with the periphery of a second phen on a neighboring tecton. The relevant distances and angles are:  $\text{Cg}\cdots\text{Cg}\cdots 3.546(2) \text{ \AA}$ ;  $\text{Cg}\perp\cdots\text{Cg}\perp\cdots 3.3495(15) \text{ \AA}$ ;  $\beta=19.17^\circ$ .

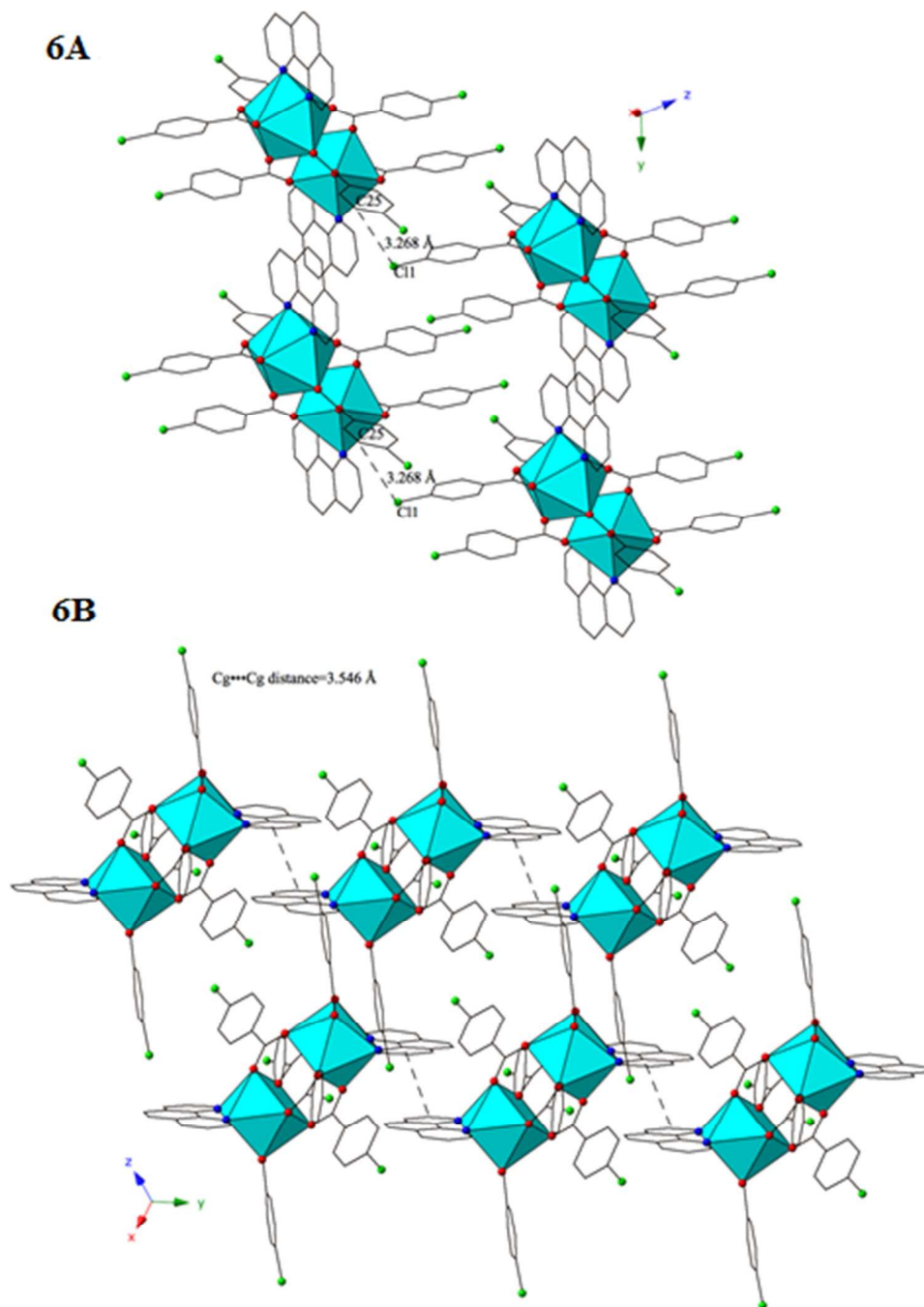


**Figure 6a)** Polyhedral representation of structure type III highlighting Cl- $\pi$  interactions that stitch together binuclear units to form 1D chain propagating in the [010] direction. **b)**  $\pi$ - $\pi$  interactions that assemble tectons into 2D sheets in the (011 plane).

### Structural Discussion

As previous Ln<sup>3+</sup>-*p*-chloro-phen studies<sup>21, 32-35</sup> have focused on the structural and spectroscopic properties of a single species, the larger structural and supramolecular trends in this series of materials have remained unexplored. The goal of this work was to synthesize all members of the RE<sup>3+</sup>-*p*-chloro-phen series from analogous starting materials and under similar reaction conditions so that the influence of the lanthanide contraction on local and global structures could be ascertained. Moreover, the resulting structures would provide a forum for the study of the influence of ionic radii on supramolecular interactions and the resulting extended solid-state assembly. White and colleagues, in their pioneering work on Ln<sup>3+</sup>-carboxylate complexes with phen and terpy,<sup>31</sup> observed subtle changes in the coordination geometry of lanthanide-phen complexes that corresponded with decreases in ionic radii. In structure types I, II and III presented herein a similar trend is observed. The RE(III) metal centers are chelated by a bidentate phen molecule, bound by *p*-chlorobenzoic acid ligands in bidentate and monodentate fashions and with the exception of La<sup>3+</sup> adopt coordination numbers of eight. The lanthanum complex (**1**) has a coordination number of nine and with an ionic radius of 1.216 Å<sup>71</sup> (compared to 1.143 Å for Ce<sup>3+</sup> with CN=8) this allows for a chelating-bridging coordination mode of the *p*-chlorobenzoic acid that is not observed in any of the other members of the Ln<sup>3+</sup>-*p*-chloro-phen series. Beyond the subtle changes in local coordination geometry of Ln-carboxylate-N-donor molecular materials that have been observed by White *et. al.* and more recently by our group,<sup>38</sup> we observed an

evolution in the supramolecular interactions (i.e  $\pi$ - $\pi$  stacking, hydrogen bonding, halogen- $\pi$ ) between binuclear molecular units, which can be correlated to local coordination geometry of the materials and is discussed below.

The local structure of all fifteen Ln<sup>3+</sup>-*p*-chloro-phen (this includes the eleven synthesized for this study and the four synthesized as part of previous works) feature both Ln-O and Ln-N bonds. The nature of the Ln-O bonds changes with structure type and observed coordination mode and details on these bond lengths and angles can be found in the Supporting Information (Table S1, SI). Ln-N bonds between the bidentate phen and the corresponding Ln(III) metal center are a constant presence throughout all fifteen structures from La-Y and this allows us to monitor the effect of the lanthanide contraction across this complete series of materials (Table 2).

Both nitrogen atoms of the phen molecule are crystallographically unique and together with the Ln<sup>3+</sup> ion provide a good source of structural data. The Ln-N bond length decreases by 6.56% for N1 and 9.04% for N2 across the Ln<sup>3+</sup> series, both of which are slight deviations from earlier studies that determined the structure for a series of compounds for all Ln metals (La-Lu) and observed bond length contractions in the 7-8% range.<sup>72-74</sup> These deviations may be a result of small steric effects from varying carboxylate binding modes, lanthanide contraction effects or differences in single crystal XRD data collection temperatures (room temp. vs. low temp.) but this has not been investigated herein in any detail. Additionally, we have observed a corresponding 8.14% increase in the N1-Ln-N2 bond angle that is also a manifestation of the lanthanide contraction.

**Table 2:** Ln-N Bond Lengths and N-Ln-N Angles in Lanthanide Complexes (**1-10**) with *p*-chlorobenzoic acid and 1,10-phenanthroline. Where complexes had been

previously synthesized (Pr, Eu, Tb and Dy) bond length data comes from corresponding CIF. Complex **11** (with Y) was omitted because yttrium is not considered part of Ln series.

f electrons (Ln <sup>3+</sup> )	d <sub>Ln-N1</sub> [Å]	d <sub>Ln-N2</sub> [Å]	∠ <sub>N1-Ln-N2</sub> [deg]
0 (La)	2.758(2)	2.743(2)	59.93(8)
1 (Ce)	2.706(3)	2.688(3)	61.17(9)
2 (Pr)	2.689(2)	2.668(3)	61.65(8)
3 (Nd)	2.678(2)	2.650(2)	61.86(8)
4 (Pm)			
5 (Sm)	2.6813(15)	2.6140(15)	62.08(5)
6 (Eu)	2.669(8)	2.593(7)	62.7(2)
7 (Gd)	2.6534(17)	2.5826(18)	62.83(6)
8 (Tb)	2.629(6)	2.566(6)	63.13(19)
9 (Dy)	2.622(4)	2.552(4)	63.54(14)
10 (Ho)	2.6148(18)	2.5405(19)	63.75(6)
11 (Er)	2.6051(18)	2.5281(19)	64.05(6)
12 (Tm)	2.594(2)	2.519(2)	64.27(7)
13 (Yb)	2.581(2)	2.509(2)	64.49(8)
14 (Lu)	2.577(3)	2.495(3)	64.81(12)
d <sub>La</sub> /d <sub>Lu</sub>	1.070	1.099	
Δ(d <sub>La</sub> →d <sub>Lu</sub> )	6.56%	9.04%	8.14%

As was mentioned previously, an evolution in the supramolecular interactions used for assembly was observed across this series of RE<sup>3+</sup>-*p*-chlorobenzoic acid-phen materials. In structure I, which was only found with the La<sup>3+</sup> ion and features a chelating-bridging carboxylate coordination mode and a bound water molecule, the binuclear units stitch together to form a supramolecular 1D chain via moderately strong, cooperative Cl- $\pi$  interactions and then are assembled into a 2D sheets via a synergistic combination of off-center  $\pi$ - $\pi$  stacking and hydrogen bonding from the bound water molecule. Structure II, which is observed for the slightly smaller Ce-Nd ions, still has a bound water molecule, yet now has two *p*-chlorobenzoic acid ligands adopting bridging bidentate coordination modes instead of the combination of chelating-bridging and bridging bidentate coordination that was observed in structure I. Structure II also forms a

supramolecular 2D sheet, yet this is done via a combination of a bifurcated hydrogen bonding interaction (originating from the bound water molecule) and offset  $\pi$ - $\pi$  stacking between phen units. Structure III predominates throughout the RE series (from Sm-Y) and, like structure types I and II, is also a binuclear molecular species. As the RE<sup>3+</sup> ions are now smaller, the 1<sup>st</sup> coordination sphere no longer contains a bound water molecule and the carboxylate coordination modes are similar to those in structure type II. A combination of strong Cl- $\pi$  and offset  $\pi$ - $\pi$  interactions assemble these materials into supramolecular 2D sheets and a systematic increase in the localized Cl- $\pi$  interaction strength, demonstrated by a decrease in Cl- $\pi$  interaction distances, is observed as the lanthanide contraction takes effect and the ionic radii of the RE<sup>3+</sup> decreases (Table S2, Supporting Information).

### Luminescence

Solid-state luminescence spectra for the Eu<sup>3+</sup> and Tb<sup>3+</sup> materials that are a part of this series have been reported previously.<sup>32, 33</sup> The praseodymium and dysprosium complexes in this series have previously been structurally characterized, yet information about their luminescent properties was not included in the earlier works.<sup>21, 34, 35</sup> Sm<sup>3+</sup> and Tm<sup>3+</sup> are known to have bands in the visible spectrum so the luminescent properties of these new isomorphs were investigated. Overall, solid-state photoluminescent spectra were collected for complexes **4 (Sm)** and **8 (Tm)** and the Pr and Dy complexes were re-made as a part of this work after sensitization by the 1,10-phenanthroline antenna.

For complex **4 (Sm)**, the characteristic  $^4G_{5/2} \rightarrow ^6H_J$  ( $J=5/2 \rightarrow 9/2$ ) transitions were observed at approximately 564, 597 and 648 nm (after excitation at 350 nm). (Figure 7) We observe a small amount of splitting of the  $^4G_{5/2} \rightarrow ^6H_{7/2}$  peak with a shoulder at 603

nm, which can be attributed to the sensitivity of this magnetic-dipole transition to its ligand environment. The  ${}^4G_{5/2} \rightarrow {}^6H_{7/2}$  peak is responsible for the orange-red emission color of Sm(III)<sup>75</sup> and is more intense than the hypersensitive  ${}^4G_{5/2} \rightarrow {}^6H_{9/2}$  electric-dipole transition at 648 nm.

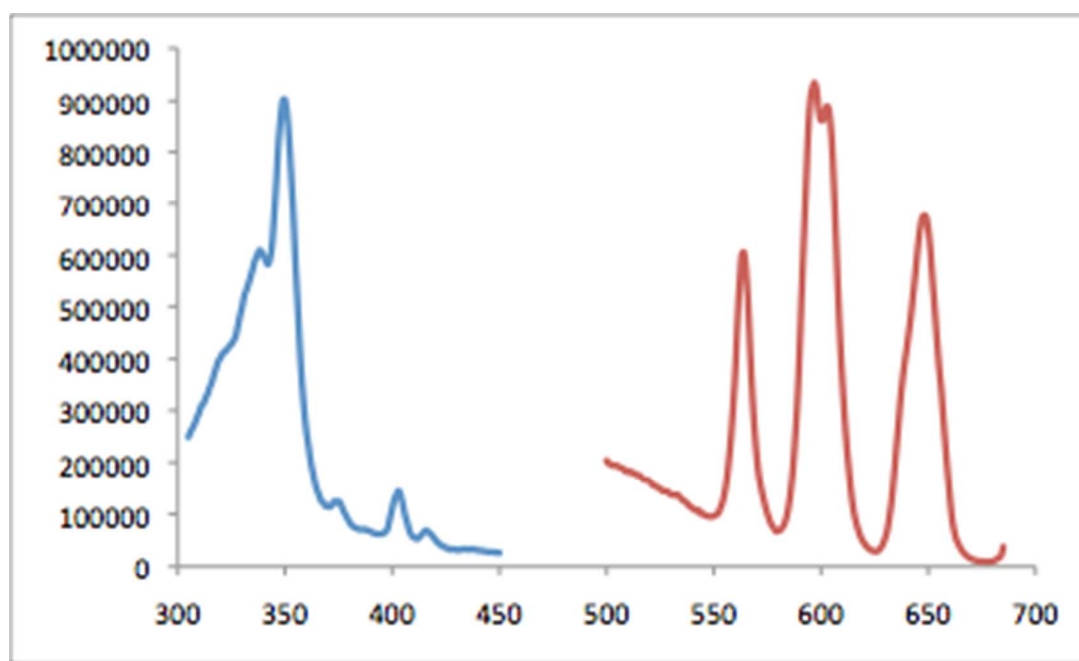


**Figure 7** Room temperature excitation and emission spectra for Sm complex 4. Excitation spectrum is the solid blue line while emission spectrum is the solid red line.

The spectrum of the Dy complex after excitation at 342 nm is shown in Figure 8. Three bands at 481, 575 and 616 nm are observed and these correspond to the  ${}^4F_{9/2} \rightarrow {}^6H_J$  ( $J=15/2 \rightarrow 11/2$ ) transitions of Dy(III), respectively. The  ${}^4F_{9/2} \rightarrow {}^6H_{13/2}$  electric-dipole transition is often the most intense peak in the visible spectrum of Dy<sup>3+</sup>,<sup>76</sup> yet here the higher energy  ${}^4F_{9/2} \rightarrow {}^6H_{15/2}$  magnetic-dipole transition is slightly more intense. This is an indication that the phen ligand is suitable for the sensitization of both the blue and yellow luminescence of the Dy(III) ion.<sup>77</sup>

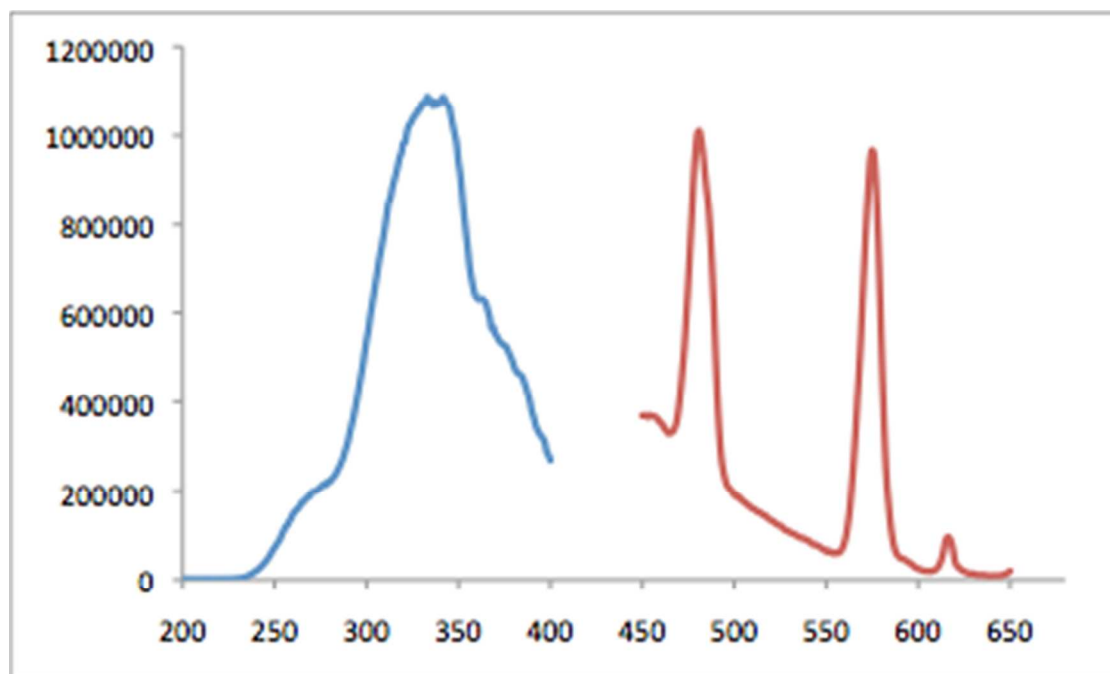


**Figure 8** Room temperature excitation and emission spectra for Dy complex.<sup>21, 35</sup> Excitation spectrum is the solid blue line while emission spectrum is the solid red line.

The visible emission spectrum for complex **8 (Tm)** was collected at an excitation wavelength of 363 nm and two small, characteristic bands corresponding to the  $^1G_4 \rightarrow ^3F_4$  transition at 592 nm and 616 nm were observed.<sup>78</sup> (Figure 9) The hypersensitive  $^1G_4 \rightarrow ^3H_6$  band expected at 450 nm was not observed as back energy transfer limits the energy transfer process from the phen ligand to the  $Tm^{3+}$  ion. Instead, we observe part of the  $^1\pi\pi_1^*$  emission band of the phen ligand,<sup>79</sup> which can be seen in Figure 9 beginning at 450 nm and then continuing to decrease in intensity until the characteristic emission band of Tm(III) is reached at 592 nm. According to Latva's energy match principle, efficient energy transfer requires a difference in triplet state energy of  $>2500\text{cm}^{-1}$  in order to avoid back energy transfer between the ligand triplet state and the lanthanide excited state.<sup>80</sup> The triplet state energy level of 1,10-phenanthroline was measured at  $22100\text{cm}^{-1}$  whereas the emitting  $^1G_4$  level of thulium is known to be at ca.  $21350\text{cm}^{-1}$ .<sup>81</sup> The difference in

these two values ( $750\text{ cm}^{-1}$ ) is well short of the  $2500\text{ cm}^{-1}$  energy gap required for efficient sensitization, so the observed  $\text{Tm}^{3+}$  luminescence in Figure 9 likely represents an example of incomplete energy transfer.

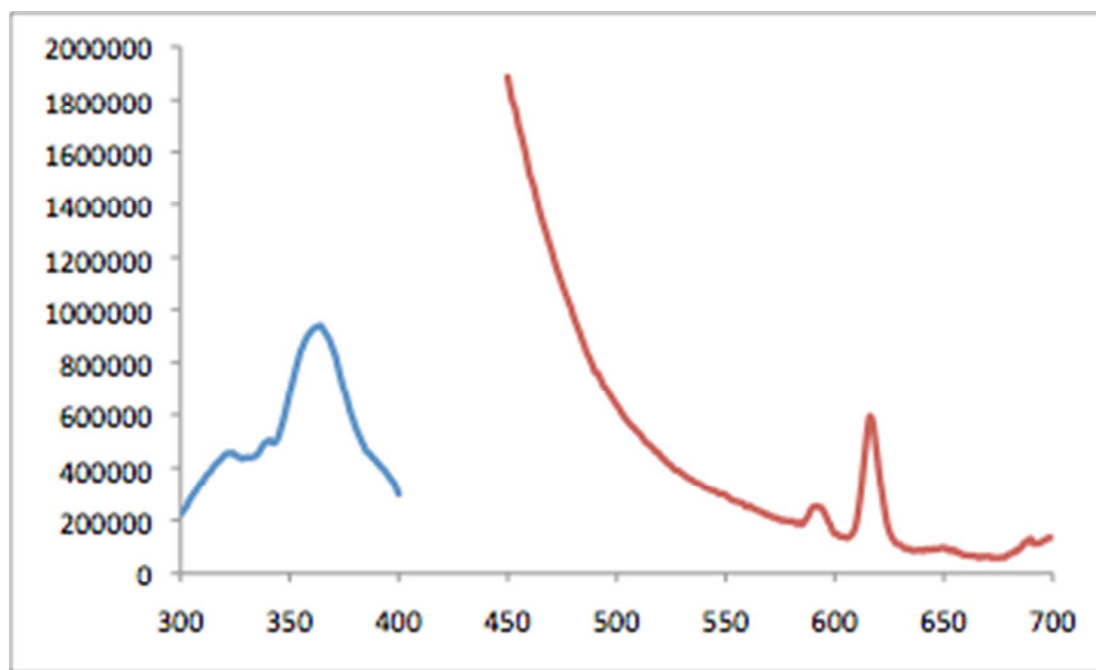


**Figure 9** Room temperature excitation and emission spectra for Tm complex **8**. Excitation spectrum is the solid blue line while emission spectrum is the solid red line.

Visible luminescence of the praseodymium complex was investigated, yet upon excitation at the absorption maxima of the phenanthroline ligand (355 nm) none was observed. The emitting  $^3\text{P}_0$  level of praseodymium is known to be at ca.  $21390\text{ cm}^{-1}$ ,<sup>81</sup> yet Hasegawa et. al.<sup>79</sup> showed that energy transfer from the triplet state of phen to praseodymium first proceeds through the non-emitting (and higher energy)  $^1\text{I}_6$  state before relaxation to the emitting  $^3\text{P}_1$  and  $^3\text{P}_0$  excited states. As the energy gap between the  $^3\text{P}_0$  state and the phen triplet state is only  $710\text{ cm}^{-1}$  this energy transfer would be considered far from efficient based on Latva's rules,<sup>80</sup> yet based on the results observed for the  $\text{Tm}^{3+}$ , it is possible that some luminescence could be detected. With the energy

transfer information provided by Hasegawa and colleagues and the consideration that the  $\text{Pr}^{3+}$  has a water molecule, a high-energy O-H oscillator in its 1<sup>st</sup> coordination sphere it is perhaps not surprising that praseodymium luminescence is completely absent.

## Conclusions

The synthesis and crystal structures of eleven rare-earth complexes containing *p*-chlorobenzoic acid and 1,10-phenanthroline obtained using hydrothermal reaction conditions have been reported, and their visible luminescent properties have been discussed. The lanthanide contraction plays a role in the observed structural changes and resulting evolution of supramolecular interactions, from a synergistic combination of halogen $\cdots\pi$ ,  $\pi$ - $\pi$  and hydrogen bonding interactions observed with La (structure type I) to a cooperative pair of  $\pi$ - $\pi$  and hydrogen bonding interactions observed for Ce-Sm (structure type II) and a combination of halogen- $\pi$  and  $\pi$ - $\pi$  interactions for Eu-Y (structure type III), that are observed as one moves across the lanthanide series. Follow up studies are looking at how changing the number of halogens on the benzoic acid group can effect the resulting supramolecular interactions of a complex and also the corresponding luminescent and magnetic properties. Functionalization of the ‘back-end’ of the phenanthroline moiety to provide additional supramolecular binding sites with imidazole and other similar groups is also ongoing.

## Supporting Information Available

X-ray crystallographic files in CIF format, ORTEP figures of all compounds, PXRD spectra of all compounds, representative low temperature single crystal XRD data and tables of selected supramolecular interaction distances and bond lengths are all available. CIFs have also been deposited at the Cambridge Crystallographic Database

Centre and may be obtained from <http://www.ccdc.cam.ac.uk> by citing reference numbers 1018738-1018748 for compounds **1-11**, respectively.

### **Author Information**

Corresponding Author

\*E-mail: [cahill@gwu.edu](mailto:cahill@gwu.edu) Phone: (202) 994-6959

Notes

The authors declare no competing financial interest.

### **Acknowledgement**

This material is based on work supported as part of the Materials Science of Actinides, an Energy Frontier Research Center funded by the U.S. Department of Energy, Office of Science, Office of Basic Energy Sciences, under Award Number DE-SC0001089. K. P. C. would also like to acknowledge George Washington University for a Presidential Merit Fellowship award. The authors would also like to thank Jessica Washner and Christine Doffek of the Seitz Group at Ruhr-University Bochum for their invaluable discussions on  $Tm^{3+}$  luminescence.

## References

1. R. Shyni, S. Biju, M. L. P. Reddy, A. H. Cowley and M. Findlater, *Inorganic Chemistry*, 2007, 46, 11025-11030.
2. X. Li, T.-T. Zhang, Z.-Y. Zhang and Y.-L. Ju, *Journal of Coordination Chemistry*, 2007, 60, 2721-2729.
3. J.-G. Wang, C.-C. Huang, X.-H. Huang and D.-S. Liu, *Crystal Growth & Design*, 2008, 8, 795-798.
4. N. M. Shavaleev, R. Scopelliti, F. Gumy and J.-C. G. Bünzli, *Inorganic Chemistry*, 2009, 48, 6178-6191.
5. M. L. P. Reddy and S. Sivakumar, *Dalton Transactions*, 2013, 42, 2663-2678.
6. Y. Cui, Y. Yue, G. Qian and B. Chen, *Chemical Reviews*, 2012, 112, 1126-1162.
7. J. Feng and H. Zhang, *Chemical Society Reviews*, 2013, 42, 387-410.
8. C.-Y. Sun, X.-J. Zheng, X.-B. Chen, L.-C. Li and L.-P. Jin, *Inorganica Chimica Acta*, 2009, 362, 325-330.
9. R. Łyszczek and L. Mazur, *Inorganic Chemistry Communications*, 2012, 15, 121-125.
10. D.-X. Xue, A. J. Cairns, Y. Belmabkhout, L. Wojtas, Y. Liu, M. H. Alkordi and M. Eddaoudi, *Journal of the American Chemical Society*, 2013, 135, 7660-7667.
11. Y. He, H. Furukawa, C. Wu, M. O'Keeffe and B. Chen, *CrystEngComm*, 2013, 15, 9328-9331.
12. Z. Guo, H. Xu, S. Su, J. Cai, S. Dang, S. Xiang, G. Qian, H. Zhang, M. O'Keeffe and B. Chen, *Chemical Communications*, 2011, 47, 5551-5553.
13. Y. He, S. Xiang, Z. Zhang, S. Xiong, F. R. Fronczek, R. Krishna, M. O'Keeffe and B. Chen, *Chemical Communications*, 2012, 48, 10856-10858.
14. J. Kido and Y. Okamoto, *Chemical Reviews*, 2002, 102, 2357-2368.
15. P. Martín-Ramos, C. Coya, Á. L. Álvarez, M. Ramos Silva, C. Zaldo, J. A. Paixão, P. Chamorro-Posada and J. Martín-Gil, *The Journal of Physical Chemistry C*, 2013, 117, 10020-10030.
16. J.-C. G. Bünzli, *Chemistry Letters*, 2009, 38, 104-109.
17. N. Tancrez, C. Feuvrie, I. Ledoux, J. Zyss, L. Toupet, H. Le Bozec and O. Maury, *Journal of the American Chemical Society*, 2005, 127, 13474-13475.
18. G.-L. Law, K.-L. Wong, K.-K. Lau, S.-T. Lap, P. A. Tanner, F. Kuo and W.-T. Wong, *Journal of Materials Chemistry*, 2010, 20, 4074-4079.
19. Y.-M. Song, F. Luo, M.-B. Luo, Z.-W. Liao, G.-M. Sun, X.-Z. Tian, Y. Zhu, Z.-J. Yuan, S.-J. Liu, W.-Y. Xu and X.-F. Feng, *Chemical Communications*, 2012, 48, 1006-1008.
20. D. N. Woodruff, R. E. P. Winpenney and R. A. Layfield, *Chemical Reviews*, 2013, 113, 5110-5148.
21. Y.-M. Song, F. Luo, Y. Zhu, X.-Z. Tian and G.-M. Sun, *Australian Journal of Chemistry*, 2013, 66, 98-104.
22. A. de Bettencourt-Dias, *Dalton Transactions*, 2007, 0, 2229-2241.
23. J.-C. G. Bünzli, *Accounts of Chemical Research*, 2006, 39, 53-61.
24. N. Sabbatini, M. Guardigli and J.-M. Lehn, *Coordination Chemistry Reviews*, 1993, 123, 201-228.
25. J.-C. G. Bünzli and C. Piguet, *Chemical Society Reviews*, 2005, 34, 1048-1077.

26. A. Bencini and V. Lippolis, *Coordination Chemistry Reviews*, 2010, 254, 2096-2180.
27. G. Anderegg, *Helvetica Chimica Acta*, 1963, 46, 2397-2410.
28. R. D. Hancock, *Chemical Society Reviews*, 2013, 42, 1500-1524.
29. F. Allen, *Acta Crystallographica Section B*, 2002, 58, 380-388.
30. A. de Bettencourt-Dias, P. S. Barber and S. Viswanathan, *Coordination Chemistry Reviews*, 2014, 273-274, 165-200.
31. C. J. Kepert, L. Wei-Min, L. I. Semenova, B. W. Skelton and A. H. White, *Australian Journal of Chemistry*, 1999, 52, 481-496.
32. L. Jin, R.-F. Wang, L. Li and S.-Z. Lu, *Journal of Rare Earths*, 1996, 14, 161-166.
33. S.-P. Wang, R.-F. Wang and J. J. Zhang, *Chinese Journal of Inorganic Chemistry*, 2007, 23, 862-866.
34. Y. Li, R. Wang, S.-Y. Niu, J. Jin and Z.-L. Wang, *Chinese Journal of Inorganic Chemistry*, 2008, 24, 1753-1760.
35. B.-S. Zhang, *Acta Crystallographica Section E*, 2006, 62, m2645-m2647.
36. C. L. Cahill, D. T. de Lill and M. Frisch, *CrystEngComm*, 2007, 9, 15-26.
37. Z. Zheng, in *Handbook on the Physics and Chemistry of Rare Earths*, eds. J. Karl A. Gschneidner, J.-C. G. Bünzli and K. P. Vitalij, Elsevier, 2010, vol. Volume 40, pp. 109-239.
38. K. P. Carter, S. J. A. Pope and C. L. Cahill, *CrystEngComm*, 2014, 16, 1873-1884.
39. Y. Li, F.-K. Zheng, X. Liu, W.-Q. Zou, Guo, C.-Z. Lu and J.-S. Huang, *Inorganic Chemistry*, 2006, 45, 6308-6316.
40. H.-M. Ye, N. Ren, J.-J. Zhang, S.-J. Sun and J.-F. Wang, *New Journal of Chemistry*, 2010, 34, 533-540.
41. G. R. Desiraju, *Angewandte Chemie International Edition in English*, 1995, 34, 2311-2327.
42. J. D. Dunitz and A. Gavezzotti, *Crystal Growth & Design*, 2012, 12, 5873-5877.
43. G. Mínguez Espallargas, L. Brammer, D. R. Allan, C. R. Pulham, N. Robertson and J. E. Warren, *Journal of the American Chemical Society*, 2008, 130, 9058-9071.
44. S. Derossi, L. Brammer, C. A. Hunter and M. D. Ward, *Inorganic Chemistry*, 2009, 48, 1666-1677.
45. H. R. Khavasi and A. Azhdari Tehrani, *Inorganic Chemistry*, 2013, 52, 2891-2905.
46. N. P. Deifel and C. L. Cahill, *Chemical Communications*, 2011, 47, 6114-6116.
47. M. B. Andrews and C. L. Cahill, *CrystEngComm*, 2013, 15, 3082-3086.
48. R. G. Surbella III and C. L. Cahill, *CrystEngComm*, 2014, 16, 2352-2364.
49. I. Csöreg, E. Weber, T. Hens and M. Czugler, *Journal of the Chemical Society, Perkin Transactions 2*, 1996, 2733-2739.
50. Z. Yin, W. Wang, M. Du, X. Wang and J. Guo, *CrystEngComm*, 2009, 11, 2441-2446.
51. H. R. Khavasi, A. Ghanbarpour and A. A. Tehrani, *CrystEngComm*, 2014, 16, 749-752.

52. B. Notash, N. Safari and H. R. Khavasi, *Inorganic Chemistry*, 2010, 49, 11415-11420.
53. B. Notash, N. Safari and H. R. Khavasi, *CrystEngComm*, 2012, 14, 6788-6796.
54. J.-C. G. Bünzli and C. Piguet, *Chemical Reviews*, 2002, 102, 1897-1928.
55. C.-B. Liu, C.-Y. Sun, L.-P. Jin and S.-Z. Lu, *New Journal of Chemistry*, 2004, 28, 1019-1026.
56. J. Ye, J. Zhang, G. Ning, G. Tian, Y. Chen and Y. Wang, *Crystal Growth & Design*, 2008, 8, 3098-3106.
57. P. Thuéry, *CrystEngComm*, 2012, 14, 8128-8136.
58. M. Yamada and F. Hamada, *CrystEngComm*, 2013, 15, 5703-5712.
59. *SAINTE*, Bruker AXS Inc., Madison, Wisconsin, USA, 2007.
60. *APEX2*, Bruker AXS Inc., Madison, Wisconsin, USA, 2008.
61. *SADABS*, Bruker AXS, Madison, Wisconsin, USA, 2008.
62. A. Altomare, G. Cascarano, C. Giacovazzo, A. Guagliardi, M. C. Burla, G. Polidori and M. Camalli, *Journal of Applied Crystallography*, 1994, 27, 435-435.
63. G. Sheldrick, *Acta Crystallographica Section A*, 2008, 64, 112-122.
64. L. Farrugia, *Journal of Applied Crystallography*, 2012, 45, 849-854.
65. A. Spek, *Acta Crystallographica Section D*, 2009, 65, 148-155.
66. *Crystal Maker*, Crystal Maker Software Limited, Bicester, England, 2009.
67. *JADE*, Materials Data Inc., Livermore, California, USA, 2003.
68. T. J. Mooibroek, P. Gamez and J. Reedijk, *CrystEngComm*, 2008, 10, 1501-1515.
69. D. Schollmeyer, O. V. Shishkin, T. Ruhl and M. O. Vysotsky, *CrystEngComm*, 2008, 10, 715-723.
70. C. Janiak, *Journal of the Chemical Society, Dalton Transactions*, 2000, 3885-3896.
71. R. Shannon, *Acta Crystallographica Section A*, 1976, 32, 751-767.
72. S. A. Cotton, V. Franckevicius, M. F. Mahon, L. L. Ooi, P. R. Raithby and S. J. Teat, *Polyhedron*, 2006, 25, 1057-1068.
73. M. Seitz, A. G. Oliver and K. N. Raymond, *Journal of the American Chemical Society*, 2007, 129, 11153-11160.
74. T. J. Boyle, L. A. M. Ottley, S. D. Daniel-Taylor, L. J. Tribby, S. D. Bunge, A. L. Costello, T. M. Alam, J. C. Gordon and T. M. McCleskey, *Inorganic Chemistry*, 2007, 46, 3705-3713.
75. S. Biju, Y. K. Eom, J.-C. G. Bünzli and H. K. Kim, *Journal of Materials Chemistry C*, 2013, 1, 6935-6944.
76. Z. Ahmed and K. Iftikhar, *The Journal of Physical Chemistry A*, 2013, 117, 11183-11201.
77. J. Xu, J. Cheng, W. Su and M. Hong, *Crystal Growth & Design*, 2011, 11, 2294-2301.
78. J. Wahsner and M. Seitz, *Inorganic Chemistry*, 2013, 52, 13301-13303.
79. M. Hasegawa, A. Ishii and S. Kishi, *Journal of Photochemistry and Photobiology A: Chemistry*, 2006, 178, 220-224.
80. M. Latva, H. Takalo, V.-M. Mikkala, C. Matachescu, J. C. Rodríguez-Ubis and J. Kankare, *Journal of Luminescence*, 1997, 75, 149-169.
81. W. T. Carnall, P. R. Fields and K. Rajnak, *The Journal of Chemical Physics*, 1968, 49, 4424-4442.

